Katholieke Universiteit Leuven

Departement Elektrotechniek ESAT-SISTA/TR 2000-2

On the Length of Subband Adaptive Filters [1]

Koen Eneman, Marc Moonen [2]

January 2000

[1]This report is available by anonymous ftp from *ftp.esat.kuleuven.ac.be* in the directory *pub/SISTA/eneman/reports/00-2.ps.gz*

[2]ESAT (SISTA) - Katholieke Universiteit Leuven, Kardinaal Mercierlaan 94, 3001 Leuven (Heverlee), Belgium, Tel. 32/16/321809, Fax 32/16/321970, WWW: *http://www.esat.kuleuven.ac.be/sista*. E-mail: *koen.eneman@esat.kuleuven.ac.be*. Marc Moonen is a Research Associate with the F.W.O. (Fund for Scientific Research – Flanders). This research work was carried out at the ESAT laboratory of the Katholieke Universiteit Leuven, in the frame of the Belgian State, Prime Minister's Office – Federal Office for Scientific, Technical and Cultural Affairs – Interuniversity Poles of Attraction Programme – IUAP P4–02 (1997–2001) : Modeling, Identification, Simulation and Control of Complex Systems, the Concerted Research Action MIPS ('Model–based Information Processing Systems') and GOA–MEFISTO–666 (Mathematical Engineering for Information and Communication Systems Technology) of the Flemish Government and Research Project F.W.O. nr. G.0295.97 ('Design and implementation of adaptive digital signal processing algorithms for broadband applications'). The scientific responsibility is assumed by its authors.

On the Length of Subband Adaptive Filters

Koen Eneman Marc Moonen
ESAT – Katholieke Universiteit Leuven
Kardinaal Mercierlaan 94, B–3001 Heverlee – Belgium
phone : +32/16321809 +32/16321060
fax : +32/16321970
email : koen.eneman@esat.kuleuven.ac.be
marc.moonen@esat.kuleuven.ac.be

Abstract

For many years now, subband adaptive filtering techniques have been proposed for the identification of high–order FIR systems. They have many desirable properties such as a low implementation cost and good convergence behaviour. However, various effects (such as residual errors and aliasing distortion) occur and reduce performance.
In this paper we will show that the complexity gain that can be obtained w.r.t. the standard fullband approach is often overestimated : the subband filters need to be longer than expected in order to model the unknown system adequately and to reduce the residual undermodelling error sufficiently.

1 Introduction

Subband adaptive schemes have been a topic of interest for many years now. They are employed to identify long FIR systems as they provide a reduced complexity solution for high–order problems and in this way outperform the standard fullband adaptive approaches. It is often suggested that subband processing leads to a considerable complexity reduction w.r.t the fullband approach, offering a complexity gain equal to the number of bands, in the limiting case where the subbands are maximally, i.e. critically downsampled. In this paper we will show that the cost reduction is often overestimated : the length of the subband filters, necessary to obtain a reliable model of the unknown system, is longer than expected and a residual undermodelling error remains. In literature many references can be found to subband adaptive filters [1]–[7].

2 Subband Adaptive Filtering : General Setup

The general setup for a subband adaptive system is shown in figure 1. The

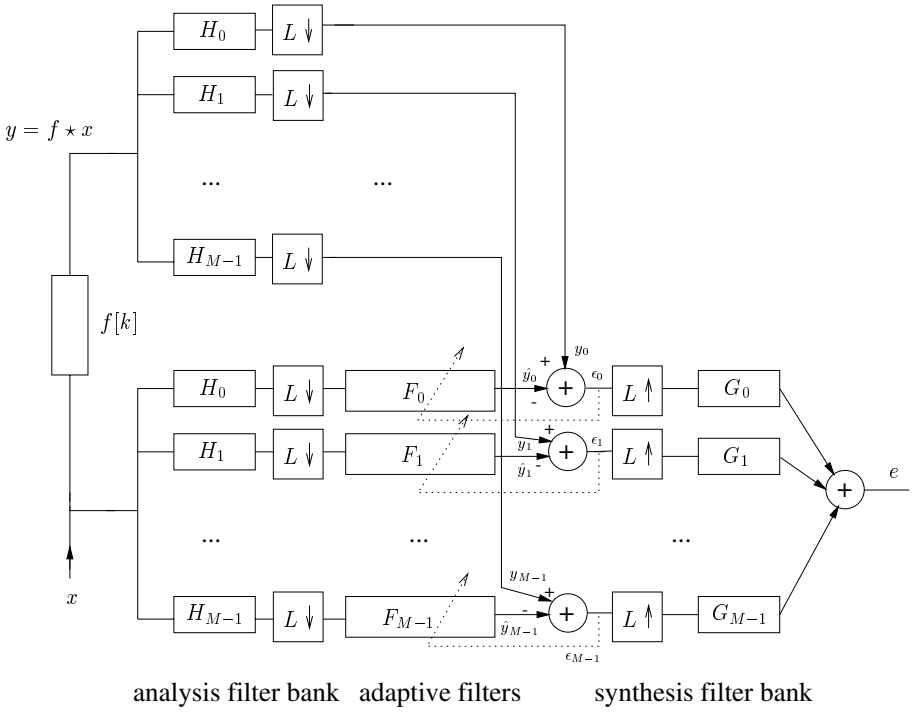

Figure 1: Subband adaptive filter : setup

input signals x and y are fed into identical M–band analysis filter banks. After subsampling with a factor L, (mostly LMS–based) adaptive filtering is done in each subband. The outputs of the subband adaptive filters are recombined in the synthesis filter bank leading to the final output e. Due to aliasing effects, this setup will only work for $M \geqslant L$.
By splitting signals into subbands and subsequent subsampling faster (initial) convergence and better tracking properties are hoped for. As the adaptive computations as well as the filter bank convolutions can be done at a reduced sampling rate, the subband approach is supposed to give a better performance at a lower cost. A subband system requires a well designed filter bank. Filter banks introduce aliasing errors (which deteriorates the adaptive filtering operations), an inherent delay and perhaps unacceptable signal distortion (non–perfect reconstruction banks).

3 Complexity Gain

The identification problem comes down to adapting M subband filters $F_i(z)$ in parallel (see figure 1) instead of just 1 filter, as in the fullband case. Very often LMS–type of algorithms are employed to adapt the subband filters as they are quite cheap. LMS adaptive filtering comes down to a combined filtering and weight updating and requires at about $2L_a$ additions and $2L_a$ multiplications per sample[1]. Subband adaptive systems are mainly based on DFT modulated filter banks, which are complex–valued. Cosine modulated filter banks [8] on the other hand are real–valued, but most of the subbands have 2 separated frequency bands : a positive and negative frequent part. After downsampling they often overlap and introduce aliasing. Aliasing will cause the convergence properties of the adaptive filters to degrade and is not desirable.
Furthermore, a DFT modulated filter bank does —roughly speaking— not lead to a more expensive implementation than a cosine modulated bank, as could be expected from first sight. In a normal setup, both the unknown system $f[k]$ as the input signal x (see figure 1) are real–valued. Hence, only half of the complex bands need to be processed as they are pairwisely complex conjugated.
Compare a DFT modulated with a cosine modulated bank having an equal number of processed bands. In the DFT case, M processed bands correspond to at about $2M$ filters. They can be downsampled at most $2M$ times leading to a cost (assuming LMS) in the order of $4L_{SB}^{\mathrm{DFT}} M \frac{1}{2M}$ complex operations per sample. L_{SB}^{DFT} is the length of the subband adaptive filters. The corresponding cosine modulated bank has M bands to be processed. They are decimated maximally M times representing a cost of $4L_{SB}^{\mathrm{DCT}} M \frac{1}{M}$ real operations per sample. As for a DFT modulated filter bank, the subbands are subsampled twice as much as for the cosine modulated bank we can assume that $L_{SB}^{\mathrm{DCT}} = 2L_{SB}^{\mathrm{DFT}}$. The difference in filter length compensates for the extra cost introduced by the complex arithmetic, which is 4 times more expensive than real arithmetic. We will now study more in detail how to choose an appropriate subband adaptive filter length L_{SB}.

4 Subband Adaptive Filter Length

Taking figure 1 and lifting out one band leads to figure 2. Suppose the unknown system can be modelled as an L_{FB}–taps FIR system $F(z)$. This implies that samples of the input channel x are related to samples of y within a time horizon of $\frac{L_{FB}}{f_s}$ seconds.[2] For a finite–length FIR system no correlation is supposed to exist between x and y beyond this horizon. After subband splitting and L–fold downsampling, the time horizon defining the intercorrelation time between x_i and y_i, is supposed to stay unchanged. As the sampling rate has been reduced with a factor L, the expected equivalent subband filter length L_{SB} to model $F_i(z)$ would —at first sight— be $\frac{L_{FB}}{L}$. For small oversampling factors, for which

[1] L_a is the length of the FIR system to be identified.
[2] f_s is the sampling frequency.

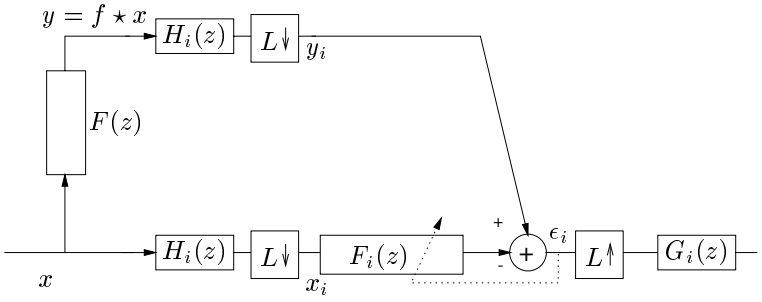

Figure 2: Adaptive filtering in subbands

$M \approx L$, the adaptive filtering cost (assuming an M–band DFT modulated filter bank and LMS updating) corresponds to $4L_{SB}\frac{M}{2}\frac{1}{L} = 2M\frac{L_{FB}}{L^2} \approx 2\frac{L_{FB}}{L}$ complex operations. The subband approach seems to be a factor $\frac{L}{2}$ cheaper than fullband processing, apart from the inherent filter bank cost of course.
This plausible reasoning, based on physical relations between x and y, is somewhat unprecise. Aliasing hampers convergence, so we choose $M > L$. But more important, it appears that L_{SB} should be taken significantly larger than $\frac{L_{FB}}{L}$ in order to lead to a satisfactory performance. One can prove (see appendix A) that in the case of an M–band, L–fold downsampled ideally frequency selective DFT modulated filter bank the i–th subband adaptive filter should converge to $\hat{f}_i[k]$:

$$\hat{f}_i[k] = \left(f[m] \star \left(e^{-j\frac{2\pi im}{M}}\mathrm{sinc}(\frac{\pi m}{L})\right)\right)_{L\downarrow}, \tag{1}$$

i.e., $\hat{f}_i[k]$ can be obtained by downsampling the convolution of the impulse response of the unknown system $f[k]$ and a modulated double–sided sinc. Even when $f[k]$ represents an FIR filter, $\hat{f}_i[k]$ in general is not FIR. The adaptive identification process therefore has to track (many) more than $\frac{L_{FB}}{L}$ samples and due to the spreading out in both directions of the time axis, an extra delay has to be inserted in the upper signal path (see figure 2).

5 Experiments

In a first example an acoustic room impulse response is considered (see figure 3). The room ($4 \times 3 \times 2.5$ meter^3) is strongly reverberant. The distance between loudspeaker and microphone is 20 cm. The response is an approximation and is generated following the method of Allen and Berkley [9]. The sampling frequency is 8 kHz. The downsampling factor is 10.
Neglecting the additional subband filter length due to these sinc–effects can strongly hamper the convergence of the adaptive filter and leads to a residual error. Extending the adaptive filter horizon in negative time direction is most effective in reducing the residual error. The anti–causal sinc–effects are

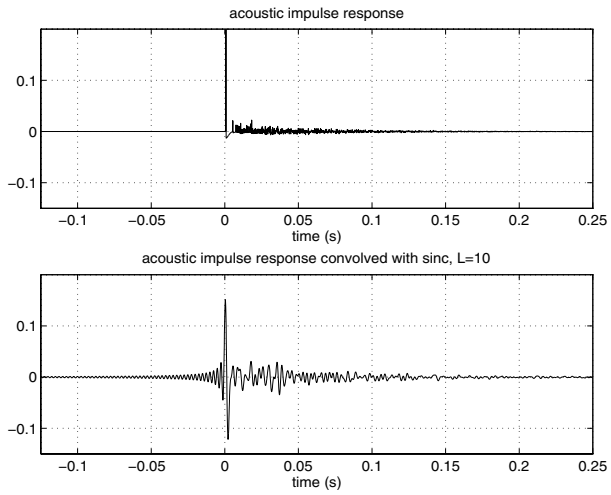

Figure 3: Impulse response (subplot 1) and the downsampled convolution with a sinc (subplot 2). The loudspeaker–to–microphone distance is 20 cm, $L = 10$.

considerable because of the small loudspeaker–to–microphone distance. In this case, the acoustic impulse response contains a dominant direct path peak and additional reverberant peaks with small and decaying amplitude. For larger microphone–to–loudspeaker distances, this effect is somewhat reduced, which is illustrated by another example (figure 4). The configuration is the same except that the distance between loudspeaker and microphone is now 150 cm.
Lowering the downsampling factor strongly reduces the amount of sinc–effects. We consider the first example again (figure 3), but now with $L = 5$ (figure 5).
In a last example we verify the theoretical results with practical data. The first (left, top) subplot shows a real acoustic impulse response obtained from measured data. In subplot 2 (right, top), the acoustic impulse response is convolved with $\text{sinc}(\frac{\pi k}{10})$. In subplot 3 (left, bottom), the downsampled version of subplot 2 is shown, corresponding to Eq. 1 ($L = 10, i = 0$). Then, the data were filtered with a sharp lowpass filter with cutoff 0.05 and were 10–fold downsampled. The impulse response between the subband data was identified and is shown in subplot 4. Apart from some measurement noise it matches the downsampled convolution which was theoretically obtained following Eq. 1 (subplot 3).

6 Conclusions

Subband adaptive schemes are used to identify high–order FIR systems as they provide a reduced complexity solution and outperform the standard fullband algorithms such as LMS. The complexity reduction which can be obtained with subband techniques is limited. The length of the subband filters needs to be

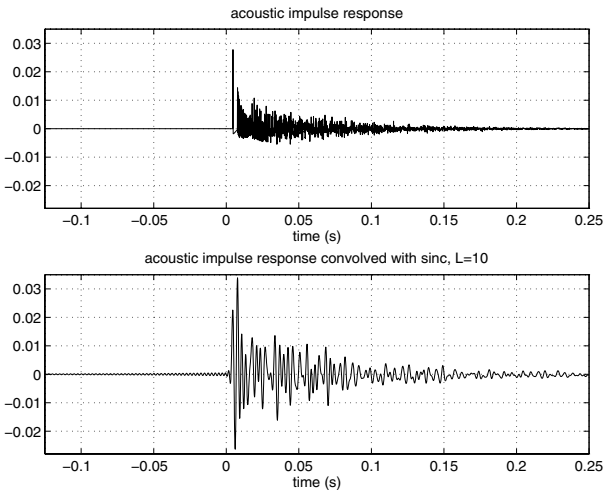

Figure 4: Impulse response (subplot 1) and the downsampled convolution with a sinc (subplot 2). The loudspeaker–to–microphone distance is 150 cm, $L = 10$.

longer than expected as extra filter taps are necessary to obtain a good model of the unknown system. Neglecting the extra delay and the additional subband filter taps strongly limits the convergence of the adaptive filters and leads to a residual undermodelling error.

7 Acknowledgements

Marc Moonen is a Research Associate with the F.W.O. (Fund for Scientific Research – Flanders). This research work was carried out at the ESAT laboratory of the Katholieke Universiteit Leuven, in the frame of

- the Belgian State, Prime Minister's Office – Federal Office for Scientific, Technical and Cultural Affairs – Interuniversity Poles of Attraction Programme – IUAP P4–02 (1997–2001) : Modeling, Identification, Simulation and Control of Complex Systems
- the Concerted Research Action MIPS ('Model–based Information Processing Systems') and GOA–MEFISTO–666 (Mathematical Engineering for Information and Communication Systems Technology) of the Flemish Government
- Research Project F.W.O. nr. G.0295.97 ('Design and implementation of adaptive digital signal processing algorithms for broadband applications')

The scientific responsibility is assumed by its authors.

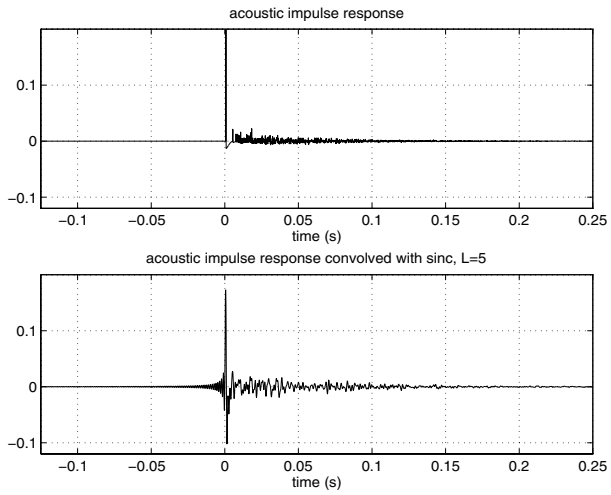

Figure 5: Impulse response (subplot 1) and the downsampled convolution with a sinc (subplot 2). The loudspeaker–to–microphone distance is 20 cm, $L = 5$.

References

[1] J. Chen, H. Bes, J. Vandewalle, and P. Janssens, "A New Structure for Sub–band Acoustic Echo Canceler," in *Proceedings of the 1988 IEEE Int. Conf. on Acoust., Speech and Signal Processing*, (New York, NY, USA), pp. 2574–2577, April 1988.

[2] W. Kellermann, "Analysis and Design of Multirate Systems for Cancellation of Acoustical Echoes," in *Proceedings of the 1988 IEEE Int. Conf. on Acoust., Speech and Signal Processing*, (New York, NY, USA), pp. 2570–2573, April 1988.

[3] A. Gilloire and M. Vetterli, "Adaptive Filtering in Sub–Bands," in *Proceedings of the 1988 IEEE Int. Conf. on Acoust., Speech and Signal Processing*, (New York, NY, USA), pp. 1572–1575, April 1988.

[4] A. Gilloire and M. Vetterli, "Adaptive Filtering in Subbands with Critical Sampling : Analysis, Experiments and Application to Acoustic Echo Cancellation," *IEEE Trans. Signal Processing*, vol. 40, pp. 1862–1875, August 1992.

[5] A. Akansu and M. Smith, *Subband and Wavelet Transforms*. Boston: Kluwer Academic Publishers, 1995.

[6] P. De León II and D. Etter, "Experimental Results with Increased Bandwidth Analysis Filters in Oversampled Subband Acoustic Echo Cancelers," *IEEE Signal Processing Letters*, vol. 2, pp. 1–3, January 1995.

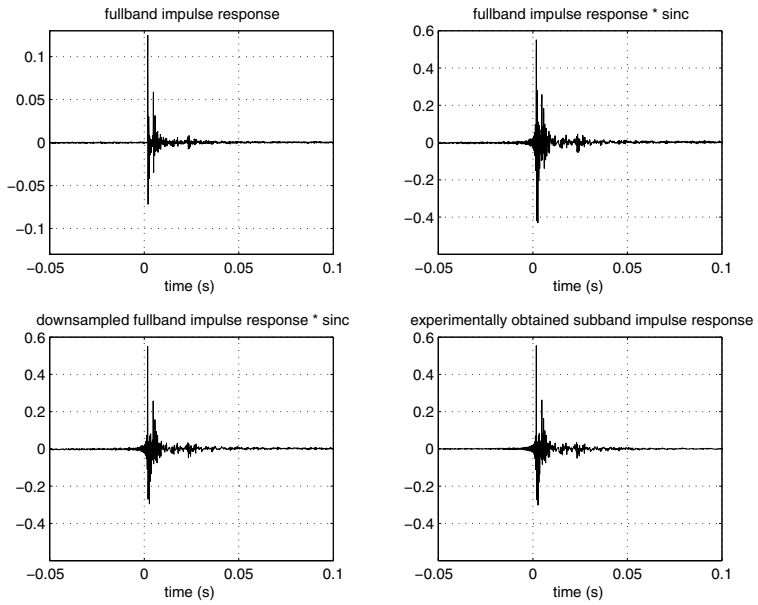

Figure 6: The first (left, top) subplot shows a real acoustic impulse response obtained from measured data. In subplot 2 (right, top), the acoustic impulse response is convolved with $\mathrm{sinc}(\frac{\pi k}{10})$. In subplot 3 (left, bottom), the downsampled version of subplot 2 is shown, corresponding to Eq. 1 ($L = 10, i = 0$). Then, the data were filtered with a sharp lowpass filter with cutoff 0.05 and were 10–fold downsampled. The impulse response between the subband data was identified and is shown in subplot 4. Apart from some measurement noise it matches the downsampled convolution which was theoretically obtained following Eq. 1 (subplot 3).

[7] D. Morgan and J. Thi, "A Delayless Subband Adaptive Filter Architecture," *IEEE Trans. Signal Processing*, vol. 43, pp. 1819–1830, August 1995.

[8] P. Vaidyanathan, *Multirate Systems and Filter Banks.* Englewood Cliffs, New Jersey, USA: Prentice Hall, 1993.

[9] J. Allen and D. Berkley, "Image method for efficiently simulating small–room acoustics," *J. Acoust. Soc. Am*, vol. 65, pp. 943–950, April 1979.

A On the Length of Subband Adaptive Filters

Call x the input to the unknown system and $y = f \star x$ the output (see figure 2), then x_i and y_i can be related to x in the Fourier domain ([8] or Eq. 4) :

$$X_i(e^{j\omega}) = \frac{1}{L} \sum_{n=0}^{L-1} H_i(e^{j\frac{\omega - 2\pi n}{L}}) X(e^{j\frac{\omega - 2\pi n}{L}}) \tag{2}$$

$$Y_i(e^{j\omega}) = \frac{1}{L}\sum_{n=0}^{L-1} F(e^{j\frac{\omega-2\pi n}{L}})H_i(e^{j\frac{\omega-2\pi n}{L}})X(e^{j\frac{\omega-2\pi n}{L}}). \quad (3)$$

$H_i(z)$ is the i–th analysis filter and in case of DFT modulated filter banks it can be written as $H_i(z) = H_0(e^{j\frac{2\pi i}{M}}z)$. Apparently, there is no simple relation between X_i and Y_i due to the frequency shifting and summation.

Lemma 1 *If the subband filters $H_i(z)$ in Eq. 2 and 3 are frequency selective i.e. the corresponding prototype filter $H_0(z)$ is capable of blocking every frequency component above $\frac{f_s}{2L}$, the L–fold downsampling will not introduce any aliasing.*

Proof : There won't be any overlap of different frequency components in this case because a complex and frequency selective DFT modulated filter bank produces subband signals having a joint, non–zero bandpass frequency spectrum with a bandwidth equal to $\frac{f_s}{L}$. This is thanks to the lowpass characteristics of the prototype filter.
In general, when a bandlimited signal s with bandwidth $\frac{f_s}{L}$ is L–fold downsampled, the subsampled signal v can be expressed as :

$$V(e^{j\omega}) = \frac{1}{L}\sum_{n=0}^{L-1} S(e^{j\frac{\omega-2\pi n}{L}}). \quad (4)$$

Aliasing would occur if for any ω in $V(e^{j\omega})$, there is more than one value of n for which $S(e^{j\frac{\omega-2\pi n}{L}}) \neq 0$.
Suppose there are 2 different values of n leading to a non–zero contribution for $V(e^{j\omega})$. $S(e^{j\Omega})$ would then be evaluated at $\Omega_1 = \frac{\omega}{L} - \frac{2\pi n_1}{L}$ and $\Omega_2 = \frac{\omega}{L} - \frac{2\pi n_2}{L}$. Hence, $\Delta\Omega = \frac{2\pi\Delta n}{L}$. One cannot find 2 different values of n for which $S(e^{j\frac{\omega-2\pi n}{L}}) \neq 0$ as we would have to evaluate $S(e^{j\Omega})$ at 2 values of Ω lying apart more than its bandwidth $\frac{2\pi}{L}$.

□

Lemma 2 *Another thing to remark in Eq. 2 and 3 is that the summation only runs over at most 2 values of n.*

Proof : L–fold downsampling in fact comes down to dividing the frequency spectrum in L equal bins. The total input spectrum is then scanned and evaluated by passing through the different bins simultaneously at a sampling rate which is L times lower and summing the results together (see figure 7 or Eq. 4). When different bins lead to scans having overlapping contributions, aliasing occurs.
The position of the n–th frequency bin is given by $\left[\frac{-1}{2L} - \frac{n}{L}, \frac{1}{2L} - \frac{n}{L}\right]$, whereas the i–th subband appears at $\left[\frac{-1}{2L} - \frac{i}{M}, \frac{1}{2L} - \frac{i}{M}\right]$. Avoiding the mirror spectra, we concentrate on $\left[-\frac{1}{2L} - 1, \frac{1}{2L}\right]$. Due to the bandlimited character of the subband signals only the bins with index $\lfloor q \rfloor$ and $\lceil q \rceil$ with

$$q = \frac{L}{M}i \quad (5)$$

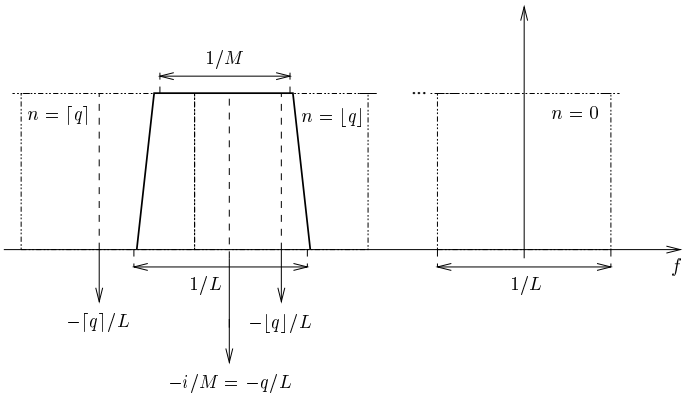

Figure 7: Downsampling mechanism

lead to non–zero contributions in Eq. 2 and 3 :

$$X_i(e^{j\omega}) = \frac{1}{L}\sum_{n=\lfloor q\rfloor,\lceil q\rceil} H_i(e^{j\frac{\omega-2\pi n}{L}})X(e^{j\frac{\omega-2\pi n}{L}}) \tag{6}$$

$$Y_i(e^{j\omega}) = \frac{1}{L}\sum_{n=\lfloor q\rfloor,\lceil q\rceil} F(e^{j\frac{\omega-2\pi n}{L}})H_i(e^{j\frac{\omega-2\pi n}{L}})X(e^{j\frac{\omega-2\pi n}{L}}) \tag{7}$$

□

In general, q is rational and there will be 2 values of n contributing. Within frame $n = \lceil q\rceil$, there is a contribution for $\frac{-1}{2L} - \frac{i}{M} < \frac{\Omega}{2\pi} \leqslant \frac{1}{2L} - \frac{\lceil q\rceil}{L}$. The downsampling process folds these back to $\lambda < \omega \leqslant \pi$, with

$$\lambda = \pi(-1 + 2\lceil q\rceil - 2q). \tag{8}$$

Similarly, frame $n = \lfloor q\rfloor$ gives a contribution for $\frac{1}{2L} - \frac{\lceil q\rceil}{L} \leqslant \frac{\Omega}{2\pi} < \frac{1}{2L} - \frac{i}{M}$, folded back to $-\pi \leqslant \omega < \lambda$. Therefore, the subband filter to identify is :

$$F_i(e^{j\omega}) = \frac{Y_i(e^{j\omega})}{X_i(e^{j\omega})} = \begin{cases} F(e^{j\frac{\omega-2\pi\lceil q\rceil}{L}}) & \text{for} \quad \lambda < \omega \leqslant \pi \\ F(e^{j\frac{\omega-2\pi\lfloor q\rfloor}{L}}) & \text{for} \quad -\pi \leqslant \omega < \lambda \end{cases} \tag{9}$$

As ω rises from $-\pi$ to π, $F(e^{j\Omega})$ is being evaluated at increasing values of Ω, except at $\omega = \lambda$ where Ω suddenly drops by $\frac{2\pi}{L}$.
The time sequence $f_i[k]$ corresponding to (9) can be found by inverse Fourier transformation :

$$f_i[k] = \frac{1}{2\pi}\int_{-\pi}^{\pi} F_i(e^{j\omega})e^{j\omega k}d\omega \tag{10}$$

$$= \frac{1}{2\pi}\int_{-\pi}^{\lambda} F(e^{j\frac{\omega-2\pi\lfloor q\rfloor}{L}})e^{j\omega k}d\omega + \frac{1}{2\pi}\int_{\lambda}^{\pi} F(e^{j\frac{\omega-2\pi\lceil q\rceil}{L}})e^{j\omega k}d\omega \tag{11}$$

$$= \frac{L}{2\pi}\int_{\frac{-\pi-2\pi\lfloor q\rfloor}{L}}^{\frac{\lambda-2\pi\lfloor q\rfloor}{L}} F(e^{j\nu})e^{j\nu(Lk)}d\nu + \frac{L}{2\pi}\int_{\frac{\lambda-2\pi\lceil q\rceil}{L}}^{\frac{\pi-2\pi\lceil q\rceil}{L}} F(e^{j\nu})e^{j\nu(Lk)}d\nu \quad (12)$$

$$= \frac{L}{2\pi}\int_{\mathcal{D}} F(e^{j\nu})e^{j\nu(Lk)}d\nu, \quad (13)$$

$$\text{with } \mathcal{D} = \left[\tfrac{-\pi-2\pi\lfloor q\rfloor}{L}, \tfrac{\lambda-2\pi\lfloor q\rfloor}{L}\right] \cup \left[\tfrac{\lambda-2\pi\lceil q\rceil}{L}, \tfrac{\pi-2\pi\lceil q\rceil}{L}\right]$$

$$= \frac{L}{2\pi}\int_{-\pi}^{\pi} G_i(e^{j\nu})e^{j\nu(Lk)}\,d\nu \quad (14)$$

$$= g_i[kL]. \quad (15)$$

$f_i[k]$ is an L–fold downsampled version of $g_i[m]$ and

$$g_i[m] = Lf[m] \star p_i[m] \quad (16)$$

in which $p_i[m]$ is a frequency clipper removing all frequency components outside $\mathcal{D}$:

$$p_i[m] = \frac{1}{2\pi}\int_{-\pi}^{\pi} P_i(e^{j\nu})e^{j\nu m}d\nu \quad (17)$$

$$= \frac{1}{2\pi}\int_{\mathcal{D}} e^{j\nu m}d\nu \quad (18)$$

$$= \frac{1}{2\pi}\frac{e^{j\nu m}}{jm}\bigg|_{\mathcal{D}} \quad (19)$$

$$= \frac{1}{2\pi}\frac{e^{j(\frac{\lambda-2\pi\lfloor q\rfloor}{L})m} - e^{j(\frac{-\pi-2\pi\lfloor q\rfloor}{L})m} + e^{j(\frac{\pi-2\pi\lceil q\rceil}{L})m} - e^{j(\frac{\lambda-2\pi\lceil q\rceil}{L})m}}{jm} \quad (20)$$

$$= \frac{1}{2\pi}\frac{e^{j(\frac{\lambda-2\pi\lfloor q\rfloor}{L})m} - e^{j(\frac{\lambda-2\pi\lceil q\rceil}{L})m}}{jm} \quad (21)$$

if $\lceil q\rceil = \lfloor q\rfloor = q$, $\mathcal{D}$ reduces to $\left[-\frac{\pi}{L} - \frac{2\pi q}{L}, \frac{\pi}{L} - \frac{2\pi q}{L}\right]$ and

$$p_i[m] = \frac{e^{-j\frac{2\pi qm}{L}}}{L}\mathrm{sinc}(\frac{\pi m}{L}) \quad (22)$$

inserting the expression for q :

$$p_i[m] = \frac{e^{-j\frac{2\pi im}{M}}}{L}\mathrm{sinc}(\frac{\pi m}{L}) \quad (23)$$

if $\lceil q\rceil \neq \lfloor q\rfloor$, $\mathcal{D}$ becomes $\left[\frac{\lambda}{L} - \frac{2\pi\lceil q\rceil}{L}, \frac{\lambda}{L} - \frac{2\pi\lfloor q\rfloor}{L}\right]$:

$$p_i[m] = \frac{e^{j\frac{m}{L}(\lambda-\pi(2\lfloor q\rfloor+1))}}{L}\mathrm{sinc}(\frac{\pi m}{L}) \quad (24)$$

$$= \frac{e^{-j\frac{2\pi qm}{L}}}{L}\mathrm{sinc}(\frac{\pi m}{L}) \quad (25)$$

$$= \frac{e^{-j\frac{2\pi im}{M}}}{L}\mathrm{sinc}(\frac{\pi m}{L}) \quad (26)$$

$$(27)$$

In both cases, $P_i(z) = P_0(e^{j\frac{2\pi i}{M}}z)$, so —as could be expected— the frequency clipper $P_i(z)$ is just a frequency translated version of the lowpass clipper $P_0(z)$. This translation corresponds to the frequency shift between H_i and H_0.
$f_i[k]$ is obtained by downsampling the convolution of the impulse response of the unknown system f and a double–sided sinc. The sinc spreads out the impulse response in both directions of the time axis. The adaptive identification process therefore has to track more than $\frac{L_{FB}}{L}$ samples and due to the spreading out in both directions of the time axis, an extra delay has to be inserted in the upper signal path.